

NUMERICAL INVESTIGATION OF THE NEAR-WALL TURBULENT CHARACTERISTICS IN STABLY STRATIFIED CHANNEL FLOW

Kyongmin Yeo

Department of Mechanical Engineering,
Yonsei University
Seoul, Korea
kyeo@yonsei.ac.kr

Changhoon Lee

Department of Mechanical Engineering,
Yonsei University
Seoul, Korea
clee@yonsei.ac.kr

ABSTRACT

To investigate the characteristics of stably stratified turbulent channel flows, direct numerical simulations of low-Reynolds number flows are performed. It is shown that the mechanism responsible for the turbulent kinetic energy is modified, although the quantity summed over the wavenumbers shows no significant changes. It is found that the dispersion in the streamwise direction is enhanced while those in the wall-normal and spanwise directions are suppressed. The Kolmogorov and buoyancy scales and model parameters such as the von K arman constant and turbulent Prandtl number are presented.

INTRODUCTION

Stratified turbulence is frequently observed in nature such as in the atmospheric boundary layer and ocean mixing layer as well as in many engineering flows. Since the stratification leads to subtle modifications of small-scale turbulent structures, overall turbulent quantities in stratified medium, including turbulent kinetic energy production, dissipation, mixing, and dispersion, differ from neutral counterparts. Therefore, the study on the stratified turbulence has been of great interest both for the physical understanding and for the engineering applications.

In stably stratified turbulence, the kinetic energy is converted into the potential energy, accompanying with the reduction of momentum, heat and scalar transport in vertical direction (Coleman et al. 1992; Holt et al. 1992; Tseng & Ferziger 2001). It has been assumed that either the co-existence of vortices and internal gravity waves or the interaction between vorticities generated by turbulence and baroclinic torque is responsible for the modification of turbulent characteristics. Metais & Herring (1989) performed direct numerical simulations (DNS) of stably stratified homogeneous turbulence. They argued that the stably stratified flows exhibit a much smaller energy transfer to smaller scales than the neutral flows and that the vortex energy at small scales decreases with increasing stability due to the reduced energy transfer. Kimura & Herring (1996) showed in their DNS of homogeneous turbulence that the vortex structures in strongly

stratified turbulence resemble scattered pancakes like the case of two-dimensional turbulence. Diamessis & Nomura (2000) found that the baroclinic torque acts as a sink which promotes decay of enstrophy in homogeneous sheared turbulence. They also suggested that the local density gradient enhances the attenuation of vertical vorticity while shear and baroclinic torque tend to maintain horizontal vorticity and it leads to the development of the pancake-type vortices. As shown above, the studies on the development of quasi-two-dimensional vortices and the related modifications of turbulent characteristics have been extensively performed in homogeneous turbulence. However, it is not straightforward to assume that the results in homogeneous turbulence can be directly applied to the inhomogeneous turbulence, particularly to turbulent boundary layer flows.

Coleman et al. (1992) showed in their DNS of turbulent Ekman layer that the turbulent quantities are seriously modified in the outer region and that the intensity and scale of vertical motions are suppressed, which in turn diminishes the production of turbulent kinetic energy. Garg et al. (2000) performed both direct numerical and large eddy simulations (LES) of stably stratified turbulent channel flows. They suggested three flow regime based on the friction Richardson number and argued that the turbulent characteristics of the outer region are different from those of homogeneous shear flows. Armenio & Sarkar (2002), however, pointed out that Garg et al. (2000) mistakenly assumed the transient state as a final state of stably stratified turbulent flows. They showed that the fluctuating motion becomes more horizontal in the log layer while the structural characteristics of turbulence shows no significant modification in the near-wall region. Iida et al. (2002) showed in their DNS of turbulent channel flows that the stable stratification selectively modifies turbulent scales: the energy spectra at low wavenumbers are attenuated while small-scale motions becomes more energetic.

The main purpose of this paper is to investigate the near-wall characteristics of stably stratified turbulent flows. For the goal, we performed DNS of stably stratified turbulent channel flows to obtain various Eulerian and Lagrangian statistics. Parameters for turbulent models are also presented.

NUMERICAL METHODS

The momentum and heat transport equations with the Boussinesq approximations are

$$\frac{\partial u_i}{\partial t} = -\frac{\partial p}{\partial x_i} + \epsilon_{ijk} u_j \omega_k - \frac{\partial}{\partial x_i} \left(\frac{1}{2} u_j u_j \right) + \frac{1}{Re_\tau} \nabla^2 u_i + Ri_\tau \theta \delta_{i2}, \quad (1)$$

$$\frac{\partial T}{\partial t} = -\frac{\partial u_i T}{\partial x_i} + \frac{1}{Pr Re_\tau} \nabla^2 T, \quad (2)$$

where x_1 , x_2 , and x_3 are the streamwise (x), wall-normal (y), and spanwise directions (z), respectively. u_i denote the corresponding velocities (u , v , w), T is temperature, and θ is fluctuating temperature. All variables in equations (1, 2) are normalized by the friction velocity u_τ , channel half-gap δ , and temperature difference between the upper and lower walls ΔT . The Reynolds, Prandtl, and Richardson numbers are defined as follows,

$$Re_\tau = \frac{u_\tau \delta}{\nu}, \quad (3)$$

$$Pr = \frac{\alpha}{\nu}, \quad (4)$$

$$Ri_\tau = \frac{\beta \Delta T g \delta}{u_\tau^2}, \quad (5)$$

where ν is kinetic viscosity, α is thermal diffusivity, and β is thermal expansion coefficient.

DNS of turbulent channel flow at $Re_\tau = 180$ and $Pr = 0.71$ was performed. The statistics are obtained for various Richardson numbers, ranging from 30 to 120. The heat and momentum transport equations are solved by a spectral method. Time was advanced by employing the Crank-Nicolson method to the viscous terms and a 3rd-order Runge-Kutta scheme to the nonlinear terms. The mean pressure gradient was kept constant to maintain the Reynolds number constant. The constant wall-temperature condition was applied for the temperature boundary condition. The computational domain is $4\pi\delta \times 2\delta \times 4\pi\delta/3$ and the corresponding grid size is $128 \times 129 \times 128$ in x , y , and z directions, respectively.

RESULTS

Eulerian statistics

The root-mean-square (r.m.s.) velocities in stably stratified turbulence are presented in figure 1. In the near-wall region ($y^+ \leq 30$), the streamwise and spanwise kinetic energies are attenuated a little while that of wall-normal direction shows no remarkable changes with increasing stability. The reduced kinetic energy in this region seems to be a result of the increase of dissipation rate. In the log-law region ($30 \leq y^+ \leq 150$), the turbulent kinetic energies in the streamwise and spanwise directions are increased while that in the vertical direction is reduced. Near the channel center, it is observed that both u^2 and w^2 are rapidly decreased.

To investigate the modification of turbulent characteristics in detail, the energy spectra are evaluated in the buffer layer (figure 2). Consistent with the observation by Iida et al. (2002), the energy contained in the large-scale motions reduces while the small-scale motions become more energetic. It is noteworthy that the crossover point in energy spectra moves toward high wavenumbers with increasing Ri_τ , indicating that

the smallest scale of motion suppressed by buoyancy becomes smaller.

Figure 3 shows vorticity fluctuations, which is closely related with the vortex structures. In the viscous sublayer, the r.m.s. vorticities are not changed by the stratification. Above the viscous layer, however, the vorticity fluctuations are intensified. In the channel center, the streamwise and wall-normal vorticity fluctuations are reduced, while the spanwise components are slightly higher than that of neutral case. This strong anisotropy seems to be caused by the internal gravity waves in the center region.

Lee et al. (2004) showed that the acceleration is intimately associated with the vortex structures. Figure 4 displays the r.m.s. accelerations. The r.m.s. accelerations are increased in almost all region. Interestingly, with increasing stability, the inflection point appearing in $\langle a_x^2 \rangle^{1/2}$ disappears (figure 4 a). This means that the pressure gradient fluctuation, which is closely related with the vortices, grows faster than the viscous forces with increasing stability (Lee et al. 2004).

Turbulent scales

The Kolmogorov length- (η) and timescales (τ_η) normalized by wall units are presented in figure 5. Both η and τ_η are decreased above the viscous sublayer unlike the case of homogeneous turbulence. However, in the center region, the Kolmogorov scales are increased, indicating that the energy is dissipated at larger scales compared to the neutral cases.

Co-existence of the coherent turbulent motions and the gravity waves is a common feature of stably stratified turbulence. An important timescale of the gravity waves is the Brunt-väisälä frequency (N). Figure 6 (a) presents N normalized by wall units. It is shown that the buoyancy timescale becomes smaller as the Richardson number increases, indicating that the smallest scale of motion affected by buoyancy becomes smaller. The Kolmogorov timescale normalized by buoyancy scale is illustrated in figure 6 (b). The ratio grows faster in the channel center region while that is insensitive in the region $y^+ \leq 120$.

Dispersion characteristics

Fluid particle dispersion is defined as follows:

$$\sigma_{X_i}^2(\tau) = \langle (X_i(t_0 + \tau) - X_i(t_0))^2 \rangle. \quad (6)$$

We evaluated the fluid particle dispersion for three initial locations; in the buffer layer, log-law region, and channel center.

Figures 7 – 9 illustrate the fluid particle dispersion normalized by δ in the streamwise, wall-normal, and spanwise directions, respectively. It is found that the dispersion in the streamwise direction is enhanced while those of the wall-normal and spanwise directions are suppressed under the stable stratification.

Considering the fact that the mean streamwise velocity is largely increased under stable stratification, the increased σ_{X_x} is an anticipated result. However, it is interesting to observe that, in the buffer layer, σ_{X_x} is increased in spite of the reduced $\langle u^2 \rangle$ and invariant mean velocity in that region, while σ_{X_z} is suppressed a little. A possible explanation for this phenomenon is that, in stably stratified flows, because of the intensified vortex structures (Yeo & Lee 2005), the chance for a fluid particle to be entrapped into the vortical structures whose convection velocities are faster than the ambient flow

in the buffer layer is increased, which eventually enhances σ_{Xx} in that region and reduces σ_{Xz} at the same time.

Consistent with the results in the homogeneous turbulence (Kimura & Herring 1996), σ_{Xy} is attenuated with increasing stability. However, the high-frequency oscillations are not observed, probably because of the relatively low Ri_τ in our simulation. Shown in the previous sections, the effects of buoyancy is the strongest in the channel center region. As a result, the suppression of wall-normal dispersion is the largest in the center region. In the center region, the fluid particles cease to move in the wall-normal direction in late times when $Ri_\tau = 90$, as reported by Kimura & Herring (1994).

Model Parameters

In the log-law region, the mean velocity gradient is approximated as follows:

$$\frac{du^+}{dy^+} = \frac{1}{\kappa y^+}, \quad (7)$$

in which κ is the von Kármán coefficient. In other words, κ can be estimated from equation (7) using data in log-law region. When $Ri_\tau = 0$, a plateau is observed in the region $40 \leq y^+ \leq 120$, as shown in figure 10. κ in the region is about 0.4. In stably stratified flows, however, the plateau is not observed. It seems that, because of the increased importance of viscosity, the log-law region is significantly reduced, consistent with the previous observation by Iida et al. (2002). However, before drawing conclusion, the simulation of higher Reynolds number flows should be performed.

Turbulent Prandtl number Pr_T is presented in figure 11. Like the neutral flows, the value of $Pr_T \simeq 1$ is observed except the channel center region. In the viscous sublayer, Pr_T shows small but gradual increase with increasing Ri_τ , which was also observed in the homogeneous flows under weak stable stratification (Armenio & Sarkar 2002). In the buffer layer, it is shown that the turbulent Prandtl numbers at various Ri_τ are well collapsed into a curve. Since the internal waves can transfer momentum but not heat, Pr_T increases markedly in the channel center region.

CONCLUSION

The Navier-Stokes equation with the Boussinesq approximation and the heat transport equation are solved to investigate the modification of turbulent characteristics under stable stratification. In the simulations, the pressure gradient was kept constant to maintain $Re_\tau = 180$. Turbulent statistics are obtained, for the Richardson number ranging from 30 to 120.

The turbulent kinetic energy in the near-wall region is not discernibly modified under the stable stratification, probably because of the strong shear in the region. The energy spectra, however, suggests that there are significant modifications of turbulent structures. Unlike velocity statistics, vorticity and acceleration fluctuations are intensified in the near-wall region, indicating that the vortical motions become more energetic. It is shown that the Kolmogorov scales are decreased in the region $5 \leq y^+ \leq 150$, while increased in the center region.

In is found that the mean-square dispersion in the streamwise direction is enhanced while those of the other two directions are reduced. The changes in the horizontal direction seem to be a combined result of the increased mean streamwise velocity and intensified vortical structures. Because of

the reduction of vertical kinetic energy, the dispersion in the wall-normal direction is significantly suppressed.

It is shown that the log-law region is reduced in the stably stratified channel flows, and hence it is difficult to estimate the von Kármán coefficient using DNS data. The turbulent Prandtl number in stably stratified flows is almost 1, like the neutral case. However, in the channel center region, due to the presence of the internal gravity waves, the turbulent Prandtl number increases rapidly.

REFERENCES

- Armenio, V. & Sarkar, S., 2002, "An investigation of stably stratified turbulent channel flow using large-eddy simulation," *J. Fluid Mech.*, vol. 459, pp. 1 – 42
- Coleman, G. N., Ferziger, J. H., & Spalart, P. R., 1992, "Direct numerical simulation of the stably stratified turbulent Ekman layer," *J. Fluid Mech.*, vol. 244, pp. 677 – 712.
- Diamessis, P. J. & Nomura, K. K., 2000, "Interaction of vorticity, rate-of-strain, and scalar gradient in stratified homogeneous sheared turbulence," *Phys. Fluids*, vol. 12 pp. 1166 – 1188.
- Garg, R. P., Ferziger, J. H., Monismith, S. G., & Koseff, J. R., 2000, "Stably stratified turbulent channel flows. I. Stratification regimes and turbulence suppression mechanism," *Phys. Fluids*, vol. 12, pp. 2569 – 2594.
- Holt, S. E., Koseff, J. R., & Ferziger, J. H., 1992, "A numerical study of the evolution and structure of homogeneous stably stratified sheared turbulence," *J. Fluid Mech.*, vol. 237, pp. 499 – 539.
- Iida, O., Kasagi, N., & Nagano, Y., 2002, "Direct numerical simulation of turbulent channel flow under stable stratification," *Int. J. Heat Mass Trans.*, vol. 45, pp. 1693 – 1703.
- Kimura, Y. & Herring, J. R., 1996, "Diffusion in stably stratified turbulence," *J. Fluid Mech.*, vol. 328, pp. 252 – 269.
- Kundu, P. K., 1990, *Fluid Mechanics*, Academic Press.
- Lee, C., Yeo, K., & Choi, J.-I., 2004, "Intermittent nature of acceleration in near wall turbulence," *Phys. Rev. Lett.*, vol. 92, art. no. 144502.
- Métais & Herring, 1989, "Numerical simulations of freely evolving turbulence in stably stratified fluids," *J. Fluids Mech.*, vol. 202, pp. 117 – 148.
- Tseng, Y.-H. & Ferziger, J. H., 2001, "Mixing and available potential energy in stratified flows," *Phys. Fluids*, vol. 13, pp. 1281 – 1293.
- Yeo, K. & Lee, C., 2005, "Modification of near-wall turbulent characteristics under stable stratification," 6th KSME-JSME Thermal and Fluid Engineering Conference, Jeju, Korea

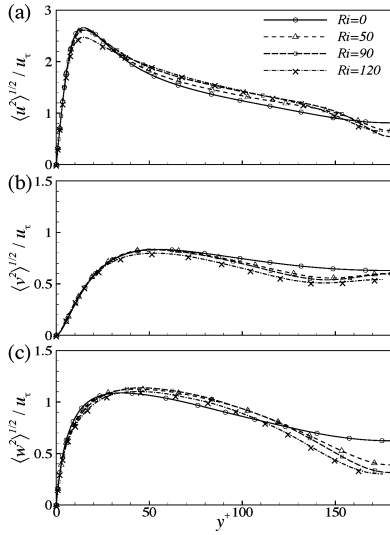


Figure 1: Root-mean-square values of (a) streamwise, (b) wall-normal, and (c) spanwise velocities.

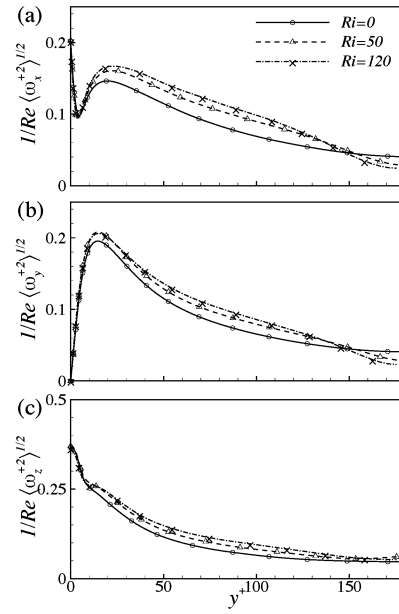


Figure 3: Root-mean-square vorticities: (a) streamwise, (b) wall-normal and (b) spanwise vorticity fluctuations.

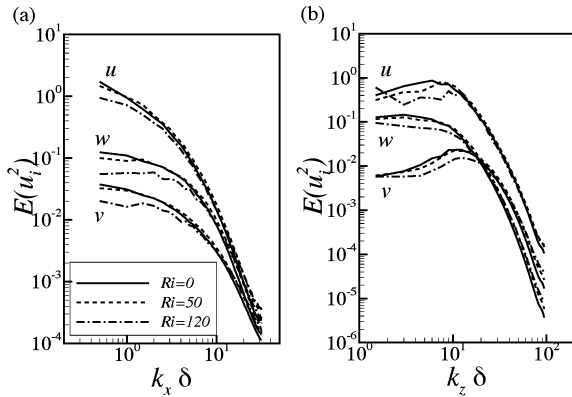


Figure 2: Energy spectra obtained at $y^+ \simeq 20$: (a) streamwise and (b) spanwise energy spectra.

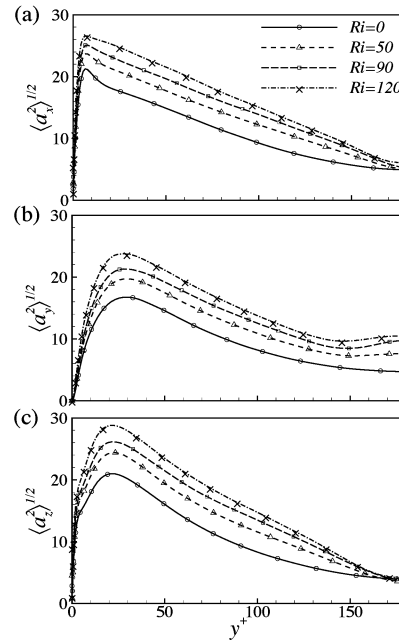


Figure 4: Root-mean-square accelerations: (a) streamwise, (b) wall-normal and (b) spanwise accelerations.

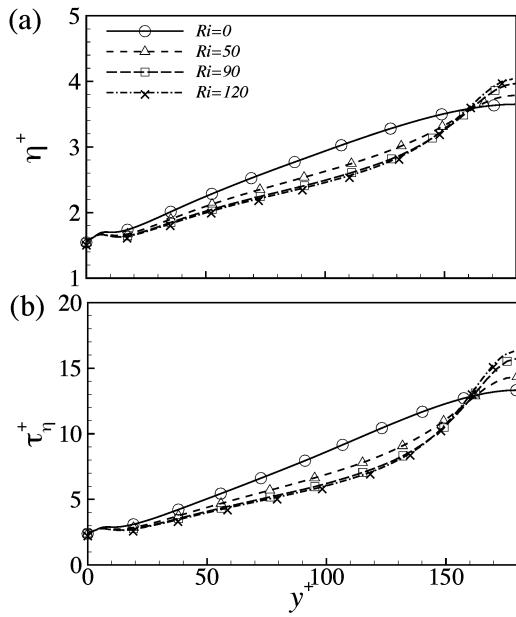


Figure 5: (a) Kolmogorov lengthscale and (b) Kolmogorov timescale normalized by wall units.

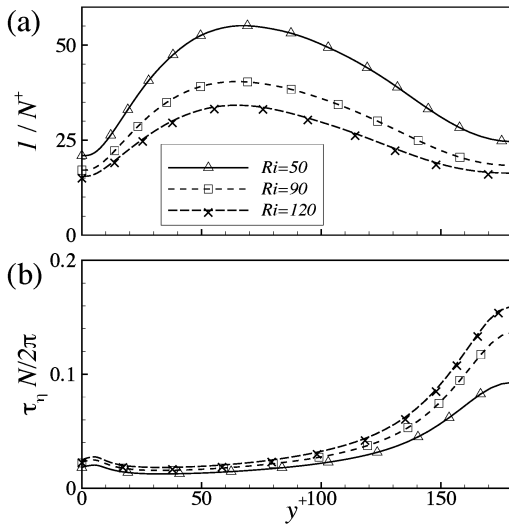


Figure 6: (a) Buoyancy timescale and (b) Kolmogorov timescale normalized by buoyancy timescale.

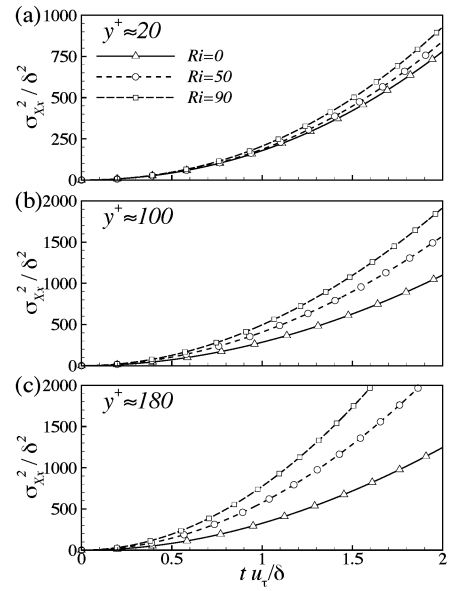


Figure 7: Fluid particle dispersion in the streamwise direction normalized by δ ; initial locations are (a) $y^+ \simeq 20$, (b) $y^+ \simeq 100$, and (c) $y^+ \simeq 180$.

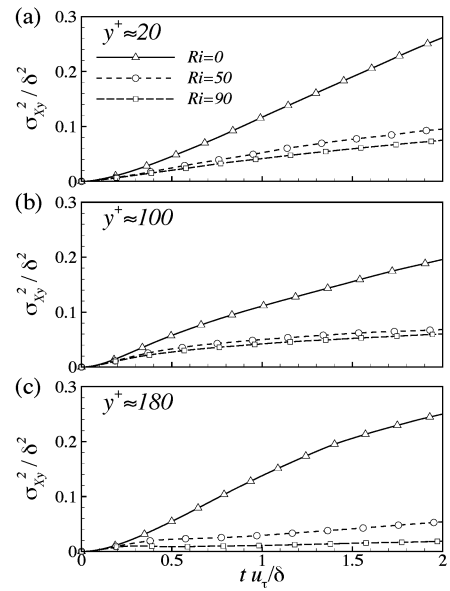


Figure 8: Fluid particle dispersion in the wall-normal direction normalized by δ ; initial locations are (a) $y^+ \simeq 20$, (b) $y^+ \simeq 100$, and (c) $y^+ \simeq 180$.

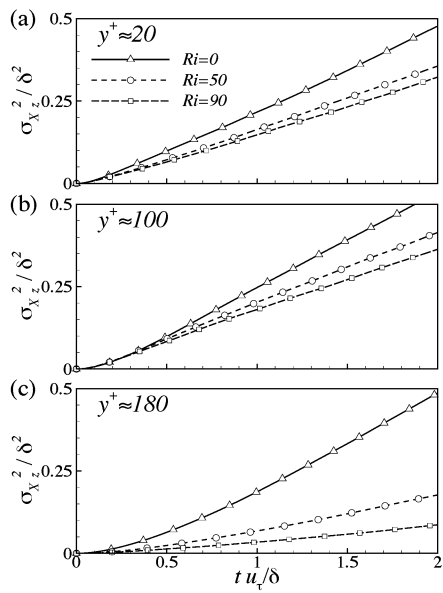


Figure 9: Fluid particle dispersion in the spanwise direction normalized by δ ; initial locations are (a) $y^+ \simeq 20$, (b) $y^+ \simeq 100$, and (c) $y^+ \simeq 180$.

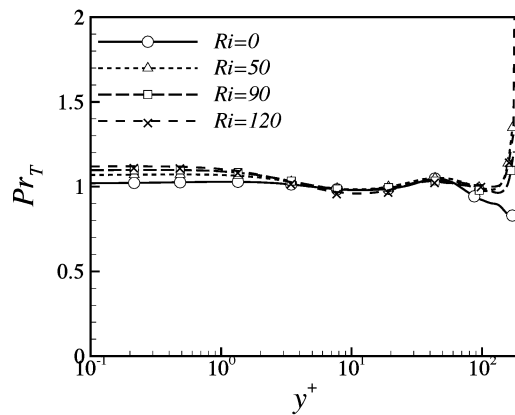


Figure 11: Turbulent Prandtl numbers estimated from DNS data.

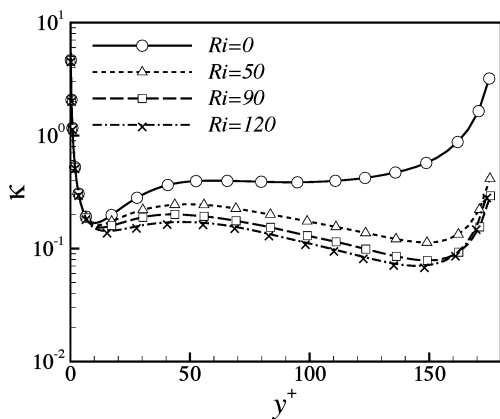


Figure 10: von Kármán coefficient estimated from DNS data.